ARTICLE

Preparation and Performance of *Pueraria lobata* Root Powder/Polylactic Acid Composite Films

Shuang Zhao[1], Shenglan Chen[2], Shuan Ren[1], Gang Li[3], Ke Song[1,4], Jie Guo[1,4], Shima Liu[1,4], Jian He[1,4] and Xianwu Zhou[1,4,*]

[1]Key Laboratory of Hunan Forest Products and Chemical Industry Engineering, Jishou University, Zhangjiajie, 427000, China

[2]Central South Inventory and Planning Institute of National Forestry and Grassland Administration, Changsha, 410000, China

[3]School of Civil Engineering and Architecture, Jishou University, Zhangjiajie, 427000, China

[4]College of Chemistry and Chemical Engineering, Jishou University, Jishou, 416000, China

[*]Corresponding Author: Xianwu Zhou. Email: zhouxianwu@jsu.edu.cn

ABSTRACT

Petroleum-based materials, such as plastic, are characterized by adverse environmental pollution; as a result, researchers have sought alternative degradable plastics that are environmentally friendly, such as polylactic acid (PLA). PLA has shown great potential to replace petroleum-based plastics. In this study, seven different samples of unmodified *Pueraria lobata* root powder (PRP) with different contents (i.e., 0, 5, 10, 15, 20, 25, and 30 wt%) and three different modified PRPs (i.e., treated with NaOH, NaOH-KH-550, and Formic) were used to reinforce polylactic acid (PLA) via solution casting process. These prepared PRP/PLA composite films were characterized using SEM, FTIR, UV-visible spectra analysis, TG, DSC, weight loss measurement (wt%), and mechanical measurements. The results showed that the PRP modified with KH-550 (PRPK) intensified the interaction in the interface region between the PRP and the PLA matrix, thus increasing the tensile strength (54.5 MPa), elongation at break (2.8%), and Young's modulus (3310 MPa) of the PRPK/PLA biofilms. Contact angle measurement showed that the PRP treatments contributed to the hydrophobicity of films. The transparency of PRP-10/PLA film at λ_{800} was 11.09%, and its *UVA* and *UVB* transmittance were 3.28 and 1.16, respectively. After blending PLA with PRP, the PRP/PLA composite films exhibited excellent biodegradability. In summary, PRPK improved the mechanical properties of PLA and prevented the films from ultraviolet light, suggesting that PRPK-5/PLA film could be used as packaging materials.

KEYWORDS

Pueraria lobata root powder; polylactic acid; biocomposite films; properties

Nomenclature

PRP	*Pueraria lobata* root powder
KH-550	3-aminopropyl triethoxysilane
PRPNa	PRP modified with NaOH
PRPK	PRPNa modified with KH-550
PRPF	PRP modified with Formic

UV	Ultraviolet
FTIR	Fourier-transform infrared spectroscopy
SEM	Scanning electron microscope
TG	Thermogravimetric
DSC	Differential scanning calorimetry
PLA	Polylactic acid

1 Introduction

In 2021, Shanghai Jiao Tong University and Science magazine published 125 of the world's most cutting-edge scientific questions, including "Can we create an environmentally friendly alternative to plastic?". According to the article, approximately 8.3 billion tons of plastics have been produced worldwide in the past 70 years. However, most of the plastics produced are non-degradable petroleum-based plastics, and 91% of them are not recyclable, resulting in severe environmental pollution. In recent years, Europe and China have proposed many policies to solve plastic pollution and actively promote biodegradable plastics while "banning plastic" [1,2]. Bio-based plastics are renewable and degradable; thus, they are an excellent alternative to petroleum-based plastics. In addition, they are one of the most effective solutions to the "white pollution" problem caused by petroleum-based plastics [3,4].

Polylactic acid (PLA) is a biocompatible, non-toxic, thermoplastic, renewable, and fully biodegradable bio-based plastic; it is widely used in apparel, packaging, agriculture, and medicine [5,6]. PLA is synthesized from lactic acid through fermentation of the starch of corn, sugar beets, and potatoes [7–10]. PLA can be decomposed into water and carbon dioxide by composting and then reintroduced into plants through photosynthesis for carbon recycling [11]. However, compared with traditional petroleum-based plastics, PLA is characterized by high production costs and relatively poor mechanical properties, significantly limiting its application [12–14]. Thus, cost reduction of PLA and improvement of its mechanical properties are essential for developing PLA products.

Currently, PLA properties can be mainly improved through chemical and physical methods. Physical modification primarily refers to the blending modification of materials, which is classified according to the different blending materials. Blending modification can include plasticizer blending, nucleating agent blending, natural fiber blending, and other degradable materials blending [15]. Among them, natural fibers can be blended with PLA to prepare composite materials owing to their renewable, low cost, low density, and high specific strength properties. The advantages of natural fibers can be fully maximized when they are blended with PLA and uniformly dispersed in PLA [16]. The modification of PLA with natural fibers can reduce the cost of PLA products and, at the time, improve their mechanical properties, crystallization rate, and gas barrier. Meanwhile, natural fibers are biodegradable and do not pollute the environment [17]. The preparation of composite materials using natural plant fibers blended with PLA for producing bio-based plastics has attracted considerable scholarly attention in recent years.

Recently, research on natural plant fiber/PLA composites mainly focused on the selection of natural plant fibers. In the past two decades, scholars from various countries have blended raw plant fiber materials, such as hemp, leaf, fruit/seed, stem, grass, and wood, with PLA for preparing composite films [9]. They found that the structure, properties of plant fibers, and the amount of plant fiber blended with PLA influenced the performance of PLA composite films. Silva et al. found that Young's modulus of the composite films increased with fiber content. In addition to the selection of plant fibers, the interfacial bonding between plant fibers and PLA is another vital influencing factor on the performance of the composite films [18]. There are numerous hydrophilic groups, such as hydroxyl groups, on the surface of plant fibers. Owing to the hydrophobicity nature of PLA, blending such plant fibers with PLA can result in poor interfacial compatibility. The poor interfacial compatibility and dispersion make the resulting

composite films unable to achieve the desired mechanical properties or make the films inferior to the unmodified PLA materials [19]. The above problems can be solved by pretreating the plant fibers. Gisan et al. found that NaOH treatment can improve the tensile strength and water resistance of PLA/durian husk fiber bio-films [20]. Silva et al. compared the effects of different modifiers on the properties of *Eucalyptus* fiber/PLA composite films. They found that the *Eucalyptus* fiber modified with surfactant had the best strengthening effect on PLA [18]. In addition to pretreatment, fibers can be modified through grafting, acylation, silylation, and oxidation.

Pueraria lobata root is a deciduous perennial vine of the genus *Pueraria* in the legume family Leguminosae. It is a medicinal and edible plant in eastern and southern Asia [21]. Starch is mainly extracted from *Pueraria lobata* root. However, every 8 kg of *Pueraria lobata* flour extracted will produce approximately 100 kg of *Pueraria lobata* waste residue. Only a smaller portion of these residues are used as feed, paper, and edible fungal medium. Most *Pueraria lobata* wastes are often landfilled or burned as waste [22], resulting in an enormous waste of resources. *Pueraria lobata* is rich in fiber content, including cellulose content up to 41.05% [23], which is higher than conventional agriculture and forestry waste (e.g., rice husk 35% [24] and straw 32% [25]). Therefore, the rational development of such cellulose-rich raw materials can effectively minimize environmental pollution caused by conventional incineration of cellulose waste and provide a theoretical reference for recycling agroforestry waste.

In this study, to minimize a large amount of high-quality *Pueraria lobata* root fiber wastes and solve the problem of the poor interfacial compatibility of plant fiber/PLA composites, *Pueraria lobata* root powder (PRP)/PLA composite films were prepared via the solution casting method. The effects of different contents (0, 5, 10, 15, 20, 25, and 30 wt%) of PRP and different modifiers (NaOH, KH-550, and formic) treated with PRP on the bio-based composite films were investigated. The film properties were examined using a thermogravimetric analyzer (TGA, NETZSCH STA 449F3, Germany), differential scanning calorimetry (DSC, TA dsc250, America TA), Scanning electron microscope (SEM, QUANTA FEG 450, FEI, America), contact angle, and water absorption tests, and the results were discussed. This study provides a theoretical basis for improving the performance of PLA products and the efficient comprehensive utilization of PRP, alleviating the problem of "white pollution".

2 Material and Methods

2.1 Materials

Pueraria lobata root was obtained from Hunan Zhangjiajie Jiu Tian Biotechnology Co., Ltd. (China). Poly (lactic acid) (PLA) (4032D) was obtained from Nature Works. Sodium hydroxide (NaOH, ≥96%, AR), 3-aminopropyl triethoxysilane (KH-550, 98%, RG), dichloromethane (CH_2Cl_2, ≥99.5%, AR), formic acid (≥98%, AR), and acetic acid (≥99.5%, AR) were purchased from General-Reagent, Shanghai. All the chemical products were used as received without further purification. Deionized water was used for all the experiments.

2.2 Preparation and Modification of PRP

2.2.1 Preparation of PRP

PRP mixture was prepared from the *Pueraria lobata* root through mechanical treatment using a miniature plant shredder (FZ102) to reduce the PRP size. Milled powder was sieved to select the size (below 0.075 mm).

2.2.2 Modification of PRP with NaOH

Precisely, 5.0 g of PRP was slowly added into 100 ml of NaOH solution (2.5 wt%) with an ultrasonic cleaner (XO-5200DT) sonicated at 250 W and 45°C for 1 h. After the reaction, the excess NaOH was rinsed

with deionized water until the solution became neutral. The rinsed PRP was freeze-dried until the excess water was removed. Afterward, the sample was dried for 24 h (SCIENTZ-10ND, Ningbo, China).

2.2.3 Modification of PRP with Formic

PRP (5.0 g) was added into a conical flask containing 100 ml of 88% formic acid solution. Then, the conical flask was transferred into a water bath and stirred at 90°C for 5 h. After the reaction, the PRP was filtered, then rinsed the formic acid on the surface with deionized water, and finally freeze-dried for 24 h (SCIENTZ-10ND, Ningbo, China).

2.2.4 Modification of PRP with KH-550

Initially, 2 wt% of KH-550 was mixed with 50 ml of ethanol (95 wt%) at 25°C. Afterward, the pH of the solution was adjusted with acetic acid to 4.5–5.5. The reaction mixture was stirred for 1 h with a magnetic stirrer to obtain the modifier agent. Then, 5.0 g of PRPNa was added to the obtained modifier agent under magnetic stirring for 2.5 h. Afterward, the silane coupling agent solution was rinsed with deionized water and freeze-dried for 24 h (SCIENTZ-10ND, Ningbo, China).

2.3 Fabrication of PLA Composite Films

The PRP/PLA films were prepared via the solvent-casting method following the reported procedure of Wang et al. [26]. PLA pellets were first dissolved in dichloromethane and stirred for 3 h at room temperature until the pellets were fully dissolved. Then, the resulting polymer solution was added to the PRP solution (prepared by dissolving PRP in 5 mL of dichloromethane) with continuous stirring at room temperature for 7 h. Subsequently, the solution was cast evenly into a glass petri dish and covered to allow slow evaporation at room temperature for at least 24 h. Pure PLA and PRP/PLA films were prepared using the same method. All composites were prepared under identical ambient conditions. Table 1 shows the individual compositions of the prepared bio-films.

Table 1: Sample compositions

Materials code	Composition		
	PLA (wt%)	PRP (wt%)	Surfactant treated
Pure PLA	100	0	–
PRP-5/PLA	95	5	–
PRP-10/PLA	90	10	–
PRP-15/PLA	85	15	–
PRP-20/PLA	80	20	–
PRP-25/PLA	75	25	–
PRP-30/PLA	70	30	–
PRPNa-5/PLA	95	5	NaOH
PRPK-5/PLA	95	5	NaOH, KH-550
PRPF-5/PLA	95	5	Formic

2.4 Characterization of PRP and PLA Composite Films

2.4.1 Thickness and Density Measurement

A micrometer (CH-1-ST, Shanghai Liuling Instrument Factory, China) was used to determine the thicknesses of the films. All the test specimens were cut into 30 mm × 30 mm rectangle strips. At least eight samples for each addition of film were tested, and every sample was measured at 10 random locations.

The film weight was measured using a Shimadzu ATX 224 analytical balance. The micrometer digital vernier caliper was used to measure the thickness, length, and width of films. All films were measured at 10 random positions to obtain 10 readings of the thickness. The film density of three samples of each PRP addition was calculated using the following formula:

$$Film\ Density = \frac{Film\ weight\ (g)}{Film\ area\ (cm^2) \times thickness\ (cm)} \tag{1}$$

2.4.2 Fourier-Transform Infrared Spectroscopy (FTIR) Measurement

The surface chemical groups of different PRP were characterized using an FTIR spectrometer. An appropriate amount of PRP, PRPK, PRPF, and PRPNa powder pressed tablets with potassium bromide (KBr) after drying was tested using FTIR (Nicolet-iS10, Thermo Scientific, USA). The infrared spectra of the samples were recorded in the range of 4000–500 cm^{-1}.

2.4.3 Thermogravimetric Analysis (TGA) Measurement

The thermal degradation behavior of pure PLA and composite films was examined using a TGA (NETZSCH STA 449F3, Germany). The films (8.0 mg) were placed in an aluminum crucible and heated from 30°C to 200°C at a scan rate of 10°C/min under a nitrogen atmosphere at a 10 mL/min flow rate.

2.4.4 DSC Measurement

DSC was used to study the thermal properties, such as glass transition temperature (T_g), melting temperature (T_m), crystallization temperature (T_c), crystallization enthalpy ΔH_c, fusion enthalpy ΔH_m, and crystallinity of PLA-based composite films. Samples (8–10 mg) were transferred into the crucible under nitrogen gas flow. All samples were performed under two thermal cycles at a heating and cooling rate of 10 °C/min. Under the first cycle, the samples were heated from 0°C to 220°C and maintained at 220°C for 3 min to eliminate thermal history, followed by the cooling of the samples to 20°C, holding for 3 min, and heating up to 220°C again. Then, the thermal property was investigated using the second thermogram. The degree of crystallinity (X_c) was calculated using the following equation:

$$X_c(\%) = \frac{\Delta H_m}{\Delta H_m^0 \times \omega} \times 100\% \tag{2}$$

where ΔH_m is the melting enthalpy, ΔH_m^0 is the melting enthalpy of unmodified PLA (93 J/g), and ω is the weight fraction of PLA in the biocomposite films.

2.4.5 SEM Measurement

The morphological properties of the PRP and the films were examined using SEM. Before observation, the samples were coated with gold to obtain sharper images.

2.4.6 Ultraviolet (UV) Spectroscopy Measurement

The light transmittance of the obtained composite films was characterized using the UV–visible spectrophotometer (U-3900 UV-VIS spectrophotometer, 2J2-0014) with the wavelengths varied from 200 to 800 nm at a scan rate of 100 nm/min. UVA (315–400 nm) and UVB (280–315 nm) were calculated using the following equations [27]:

$$UVA = \frac{T315 + T320 + T325…T395 + T400}{18} \qquad (3)$$

$$UVB = \frac{T280 + T285 + T290 + T295 + T300 + T305 + T310 + T315}{8} \qquad (4)$$

where T is the transmittance at each wavelength.

2.4.7 Water Absorption (W_a) Measurement

The water absorption of pure PLA and composite films were determined according to ASTM D570-98 (Reapproved 2018) standard. All composite films were cut to the same size using the controlled variable method, and then the films were immersed in deionized water at 25°C for 24 h. The water absorption (W_a) was calculated using the equation:

$$W_a = \frac{W_n - W_d}{W_d} \times 100\% \qquad (5)$$

where W_d and W_n are the original dried weight and the weight after exposure, respectively.

2.4.8 Contact Angle Measurement

The surface hydrophilicity of bio-films was characterized based on contact angles, which were assessed with contact angle equipment (Theta Flex, Boilin, Sweden). Distilled water was dropped on the surface of each sample at least five different sites, and the average and standard deviation were studied.

2.4.9 Tensile Properties Measurement

The mechanical properties of films were determined using a testing machine (Model UTM6104, SUNS, China) according to ASTM D882 at room temperature at a testing speed of 2 mm/min and load cell of 450 N. The samples were cut into rectangular shapes, with the size of 40 mm × 25 mm. Five specimens per film were tested.

2.4.10 Soil Burial Degradation Test

To simulate the degradation process of the films under natural conditions, samples were cut into rectangles with the size of 50 mm × 70 mm. The samples were naturally degraded in the soil about 10 cm deep from the ground under the cypress trees of Jishou University. Samples were taken out after 40 days. After the samples were washed and dried, their weight and size were measured. The percentage of weight loss was calculated using the following equation:

$$Weight\ loss\ (\%) = \frac{W_o - W_t}{W_o} \times 100\% \qquad (6)$$

where W_o is the initial mass, W_t is the mass after degradation.

3 Results and Discussion

3.1 Thickness and Density of the Biocomposite Films

The effect of PRP on the thickness and density of the film is shown in Table 2. The thickness of the pure PLA film was 0.085 mm. When the PRP content was 30 wt%, the film thickness became 0.105 mm, and the thickness of the composite film slightly increased with the increasing content of PRP. The density of the composite film decreased with increasing PRP content. The decreased density is attributable to the lower density of PRP [28]. The modified PRP was fluffy and had low density after it was freeze-dried. Thus, the modification of PRP reduced the density of the PRP/PLA composite film.

**Table 2:** Thickness and density of PRP/PLA biocomposite films

Sample	Thickness (mm)	Density (g/cm^3)
Pure PLA	0.085 ± 0.006^a	1.237 ± 0.130^d
PRP-5/PLA	0.086 ± 0.004^a	1.228 ± 0.192^d
PRP-10/PLA	0.102 ± 0.010^{bcd}	1.074 ± 0.023^{ab}
PRP-15/PLA	0.098 ± 0.004^{bcd}	1.148 ± 0.025^{cd}
PRP-20/PLA	0.098 ± 0.003^{bcd}	1.141 ± 0.019^{cd}
PRP-25/PLA	0.100 ± 0.008^{bcd}	1.136 ± 0.075^{cd}
PRP-30/PLA	0.105 ± 0.009^{cd}	1.098 ± 0.067^{ab}
PRPNa-5/PLA	0.096 ± 0.007^{abc}	0.991 ± 0.047^a
PRPK-5/PLA	0.108 ± 0.011^d	1.015 ± 0.029^a
PRPF-5/PLA	0.091 ± 0.002^{ab}	1.000 ± 0.027^a

Note: Digitals after "±" are the standard deviations, same in the following tables.

Different characters after the provided values in the same column indicate that there is a significant difference between samples at $P < 0.05$ (Student Newman Keuls test), same in the following tables.

3.2 Chemical Structures Analysis of PRP and Its Composite Films

Fig. 1 shows the FTIR image of PRP, PRPNa, PRPF, and PRPK. There was a broad peak at 3720 to 3000 cm^{-1}, attributed to the stretching vibration of O-H groups in cellulose and lignin [28]. The band at 2920 cm^{-1} corresponded to the C-H stretching vibration in cellulose and hemicellulose, and the stretching vibration of the C=O at 1734 cm^{-1} corresponded to lignin and hemicellulose (non-cellulose) [29]. The peak at 1630 cm^{-1} was assigned to O-H bending vibration in water present in PRP. The peak at 1251 cm^{-1} confirmed the benzene ring of lignin, while the peak at 1060 cm^{-1} was assigned to C-O stretching vibration. The peak at 1027 cm^{-1} was attributed to the C-OH of the cellulose glycosidic bond.
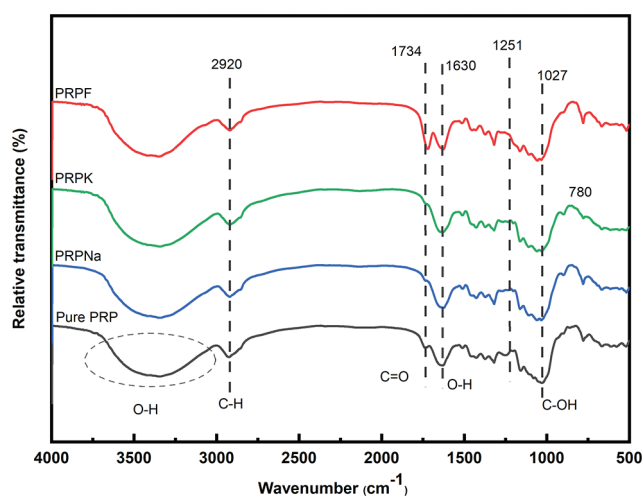
Figure 1: FTIR spectra of PRP, PRPNa, PRPK, and PRPF

The peak at 1251 cm^{-1} disappeared in PRPF, and the C=O stretching vibration peak moved from 1734 to 1721 cm^{-1} with an increase in peak intensity. These results showed that formic acid removed part of the lignin in PRP and also reacted with hydroxyl groups in PRP to form ester bonds [30,31]. The peak intensity of the PRPNa decreased at 1251 and 1734 cm^{-1}, indicating that the alkali treatment removed some impurities, such as lignin and hemicellulose, from PRP. Silva et al. also observed that alkali treatment could remove some hemicellulose and lignin in *Eucalyptus* [18]. Compared with PRPNa, no new characteristic peak was observed in PRPK (Fig. 2). However, most of the peak intensities of the PRPK (peak intensities at 3720 to 3000 cm^{-1}) were significantly higher than those of the PRPNa due to the strong hydrogen bond formed among the -OH of KH-550, PRPNa and the -NH$_2$ of KH-550 [32,33]. The characteristic absorption peak at 779 cm^{-1} was an out-of-plane bending vibration of the -NH$_2$ bond in the PRPK [34]. The above results showed that the PRP was successfully modified with alkali, formic acid, and KH-550 treatments.
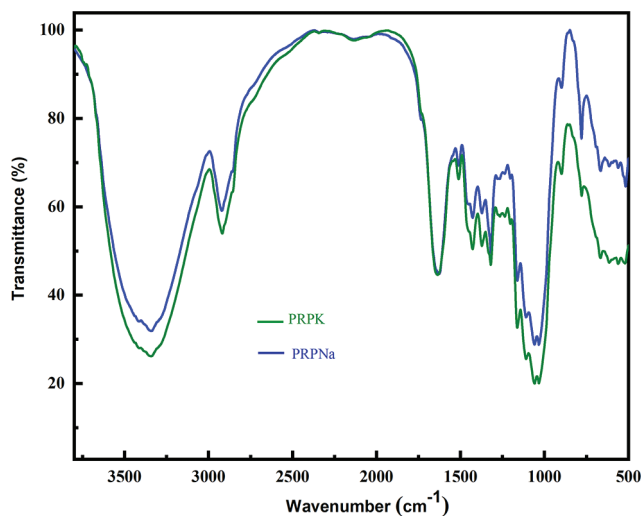

Figure 2: FTIR spectra of PRPNa and PRPK

3.3 Thermal Properties of the Biocomposite Films

Fig. 3 shows the TGA and DTG curves of the pure PLA and PLA composite films. Table 3 shows the starting degradation temperature T_{onset}, maximum degradation temperature T_{peak}, degradation 50% temperature $T_{50\%}$, ending degradation temperature T_{endset}, and residual carbon rate of different composite films determined using TGA and DTG.

As shown in Fig. 3, the initial mass loss between 45°C and 100°C was attributed to the volatilization of water contained in the composite films [35,36]. When PRP was added at 5 wt%, the T_{onset}, T_{peak}, $T_{50\%}$, and T_{endset} of the composite films did not decrease but were higher with PLA, indicating that PRP and PLA matrix bonded well. The maximum thermal decomposition temperature of PLA was 363°C, and the thermal decomposition temperature of the composite films decreased continuously with the increasing PRP content, which was attributed to the poor thermal stability of cellulose and hemicellulose compared with PLA [37]. Because alkali treatment removed most of the lignin, the thermal degradation temperature of PRPNa-5/PLA film significantly decreased [38]. The thermal degradation temperature of the PRPK-5/PLA composite film was higher than that of the PRPNa-5/PLA film, probably because the addition of a layer of KH-550 on the surface of PRP further improved the thermal stability of the composite film [39]. As shown in Table 3, the residual mass of all biocomposite films at 599°C was higher than that of PLA and increased with the increase in PRP content. This phenomenon was attributed

to the high contents of contained cellulose and lignin in PRP, which increased carbon residue at high temperatures [40].
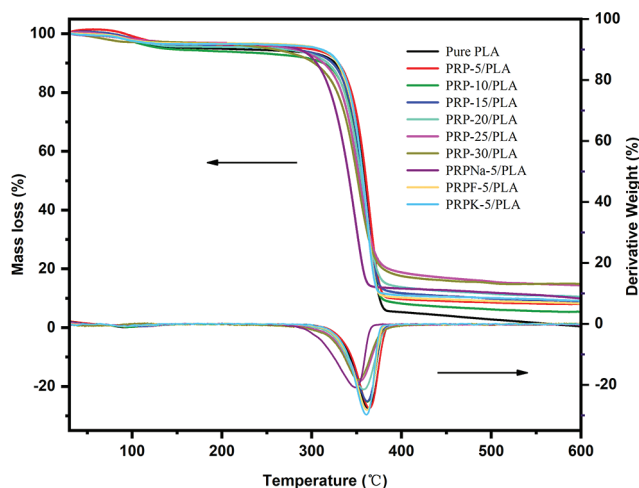

Figure 3: Thermal stability of PRP/PLA films

Table 3: TG analysis results of PRP/PLA films

Sample	T_{onset} (°C)	T_{peak} (°C)	$T_{50\%}$ (°C)	T_{endset} (°C)	Char residue (%) at 599 (°C)
Pure PLA	339	363	359	377	0.46
PRP-5/PLA	341	364	361	377	8.06
PRP-10/PLA	336	362	356	375	5.37
PRP-15/PLA	336	362	358	375	9.00
PRP-20/PLA	333	358	355	374	10.53
PRP-25/PLA	327	353	353	372	14.40
PRP-30/PLA	324	352	351	372	14.90
PRPNa-5/PLA	318	349	342	360	9.95
PRPK-5/PLA	340	361	358	371	9.13
PRPF-5/PLA	340	361	358	372	8.24

In summary, when 5 wt% of PRP was added to PLA, the thermal stability of the composite film was improved. Conversely, when PRP exceeded 5 wt%, the thermal stability of the composite film gradually decreased.

The effect of PRP on the crystallization and melting of the composite film was characterized using DSC. Fig. 4 shows that PLA is a typical semi-crystalline polymer. To eliminate the influence of processing on the experimental results, pure PLA was also processed according to the preparation of composite films before testing. The specific thermal analysis data are listed in Table 4. The glass transition of the PLA composite film was mainly attributed to physical or chemical changes in the PLA chains. The change in glass transition temperature (T_g) of the composite films with increasing PRP content was insignificant, and all curves showed a stable T_g of approximately 62°C, indicating no significant interaction between the PLA matrix and PRP. In previous reports, when micron fibers or nanoparticles were incorporated into the

polymer matrix, they acted as nucleating agents and promoted the crystallization of PLA [40,41]. However, this experiment showed the opposite result. The crystallinity of pure PLA was 61.9%, and the crystallinity of the composite film decreased after the addition of PRP. When 30 wt% of PRP was added to PLA, the crystallinity of the composite film was approximately 33.34%. These results showed that PRP promoted the amorphization of the PLA matrix [18].
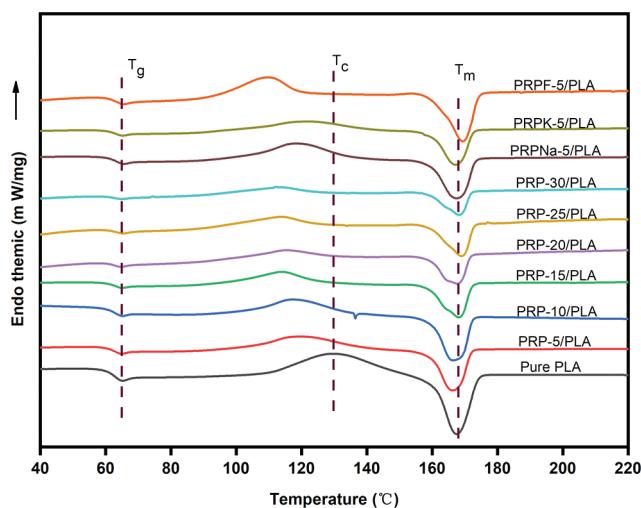

Figure 4: DSC of PRP/PLA films

Table 4: DSC analysis results of PRP/PLA films

Sample	T_g (°C)	T_c (°C)	T_m (°C)	ΔH_c (J/g)	ΔH_m (J/g)	X_c (%)
Pure PLA	62.24	129.66	167.5	65.81	57.98	61.9
PRP-5/PLA	62.19	119.63	166.32	42.48	39.29	47.63
PRP-10/PLA	61.81	118.33	166.50	42.20	42.51	50.41
PRP-15/PLA	62.11	114.00	168.16	30.76	33.43	41.97
PRP-20/PLA	62.38	115.16	167.83	27.83	27.40	36.56
PRP-25/PLA	62.87	113.83	169.00	22.25	28.97	41.22
PRP-30/PLA	62.37	112.00	168.5	14.42	21.87	33.34
PRPNa-5/PLA	62.77	109.83	167.5	34.01	45.53	51.15
PRPK-5/PLA	62.44	118.33	167.16	43.45	42.69	47.96
PRPF-5/PLA	62.41	121.16	169.3	34.79	32.76	36.80

Both alkali- and silane-treated PRP/PLA composite films showed higher crystallinity and a lower crystallization temperature than unmodified PRP/PLA composite films because alkali and silane coupling treatments promoted PRP to act as nucleating agents in the PLA matrix. The crystallinity of the PRPF-5/PLA composite films decreased, confirming that the formic acid modification increased the amorphous region of PLA [18].

3.4 Morphological Properties of PRP and Its Biocomposite Films

Fig. 5 shows SEM images of untreated PRP, PRPNa, PRPF, and PRPK. Untreated PRP contains hemicellulose, lignin, pectin, waxes, cellulose, and others. Numerous fine PRP particles were attached to the large particles of PRP. Alkali treatment removed the small PRP adsorbed on PRP, reduced the agglomeration between PRP, made PRP uniformly dispersed in the PLA matrix, made the fiber surface rougher, and closely combined PRP and PLA. The surface of PRPK was covered with a layer of nonpolar chain segments, thus making the surface of PRPK flat and smooth [33]. After PRP was treated with formic acid, the surface of PRP was very uneven, and some PRP particles were fragmented. This phenomenon was attributed to the removal of hemicellulose and lignin from PRP by formic acid [30,31], thus increasing the specific surface area of PRP and exposing more functional groups, which improved the interaction between PRP and PLA.
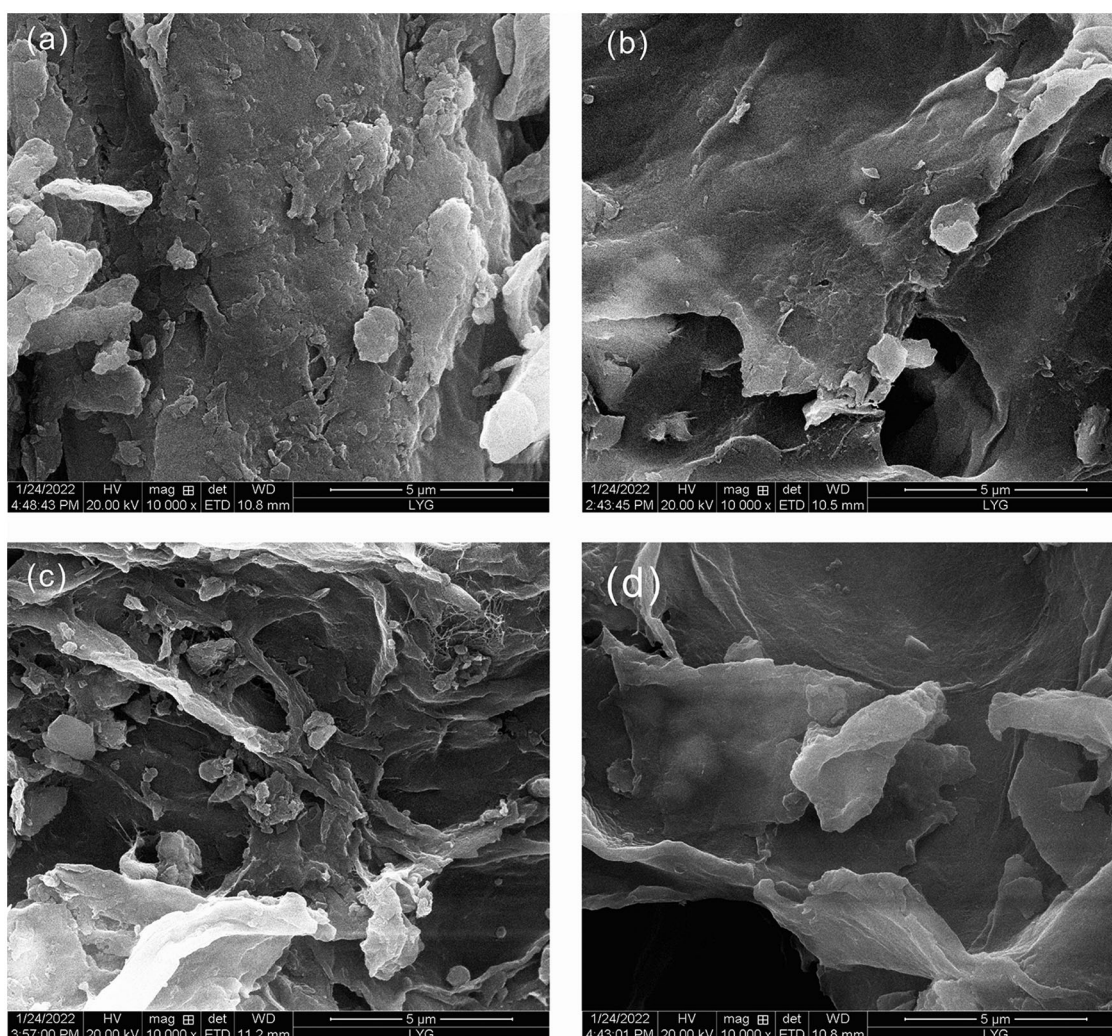

Figure 5: SEM micrographs for PRP (a), PRPNa (b), PRPF (c), PRPK (d)

Fig. 6 shows the camera, optical microscope, and SEM images of PLA film and PLA/PRP composite films with different PRP content. The camera images showed that all composite films were uniform without cracks under the visual. The pure PLA film was transparent. With the increase in PRP content,

the transparency of the composite films gradually decreased, the yellow color steadily deepened, and the roughness increased. In the optical micrograph, as the PRP content increased, the PRP was yellow, PRP/PLA composite film became darker yellow and appeared agglomerated. The SEM image revealed that the composite film exhibited a round spherical crystal structure with increasing PRP content. The spherical crystal cracked composite film [42], thus accelerating the water absorption rate of the composite film.

Fig. 7 shows the photos, optical microscope image, and SEM images of the modified PRP/PLA composite film when the PRP content was 5%. As shown in Fig. 7, the PRP before and after modification were uniformly distributed in the PLA matrix. The optical microscope of the PRPK-5/PLA composite film showed numerous black substances attached to the surface of the composite film. The KH-550 might be the substance attached to the composite film. Figs. 7a1–7c1 combined with the UV transmittance graph (Fig. 8) of the composite film show that the modified PRP did not affect the transparency of the composite film.

3.5 UV–Visible Spectra Analysis of the Biocomposite Films

Ultraviolet (UV) is exceptionally harmful to UV-sensitive products, such as food and pharmaceuticals. UV resistance is an essential indicator of UV-sensitive food and product packaging materials [43]. PLA is one of the most commonly used polymers in packaging materials; however, the weak UV-blocking properties of PLA limit its application [44]. UV radiation occurs when the sun emits wavelengths from 100 to 400 nm. The other two wavelengths of UV radiation are *UVA* (315 to 400 nm) and *UVB* (280 to 315 nm) [27]. Fig. 8 shows the UV transmittance of biocomposite films. Table 5 lists the transmittance values of *UVA* and *UVB*. The *UVA* and *UVB* of pure PLA were 93.14 and 83.68, respectively, and they were reduced to 20.58 and 15.15 when the PRP content was 5 wt%. As PRP content increased from 5% to 30%, the UV resistance of the composite film increased. This increment was ascribed to two reasons: first, the fibers absorbed UV light. Second, the increased PRP content led to mutual agglomeration and entanglement of fibers [44,45]. From Table 5, the transparency of PRP/PLA composite film modified with KH-550 was excellent, with *UVA* and *UVB* values of 13.25 and 8.61, respectively. In addition, the UV resistance of PRP/PLA was strong, which is suitable for packaging films that require transparent and UV shielding products. Therefore, PRP/PLA films have great potential application for packaging UV-sensitive products.

3.6 Water Absorption (W_a) of the Biocomposite Films

PLA composite films rapidly absorbed water after the initial mass gain and reached W_a equilibrium within 24 h. W_a of composite films was only related to the added PRP [27]. Fig. 9 shows the graphs of W_a of pure PLA and PRP/PLA composite films. As shown from the graph, the W_a of the composite films increased with the PRP content, and the W_a of the modified composite films were all lower than that of the unmodified films.

Although PLA is hydrophobic, pure PLA films gained 0.72% weight after they were immersed in deionized water for 24 h. The films gained weight because of the numerous ester groups in PLA, thus forming hydrogen bonds with water molecules [46]. The W_a of the composite films increased with the addition of PRP. When the PRP content was 5, 10, 15, 20, 25, and 30 wt%, the W_a values of PRP/PLA composite films were 0.89%, 1.93%, 2.47%, 3.24%, 5.23%, and 5.86%, respectively. The W_a of PRP-30/PLA composite film was eight times that of pure PLA. The higher W_a value of PRP-30/PLA composite film is attributable to numerous hydroxyl groups in PRP. The hydroxyl groups formed hydrogen bonds with water molecules and allowed the water molecules into the composite films, resulting in the swelling of the composite films, thus promoting the formation of a microcavity in the composite films. The resulting microcavity in the films further accelerated the infiltration of water molecules into the composite films [46–48].
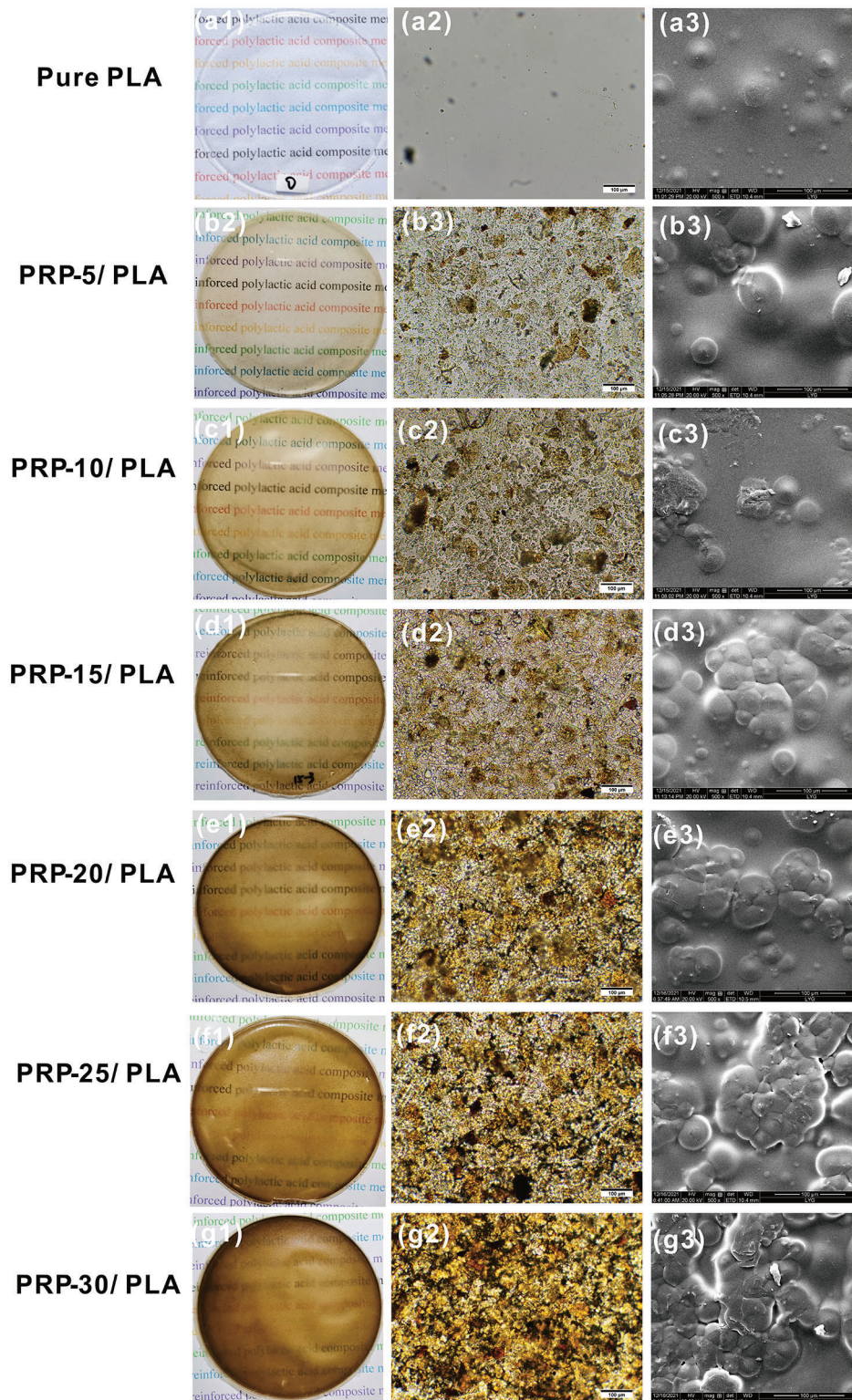
Figure 6: The camera photographs (left), optical microscope (center), and SEM image (right) of PLA film and PLA composite films with different amounts of PRP percentage
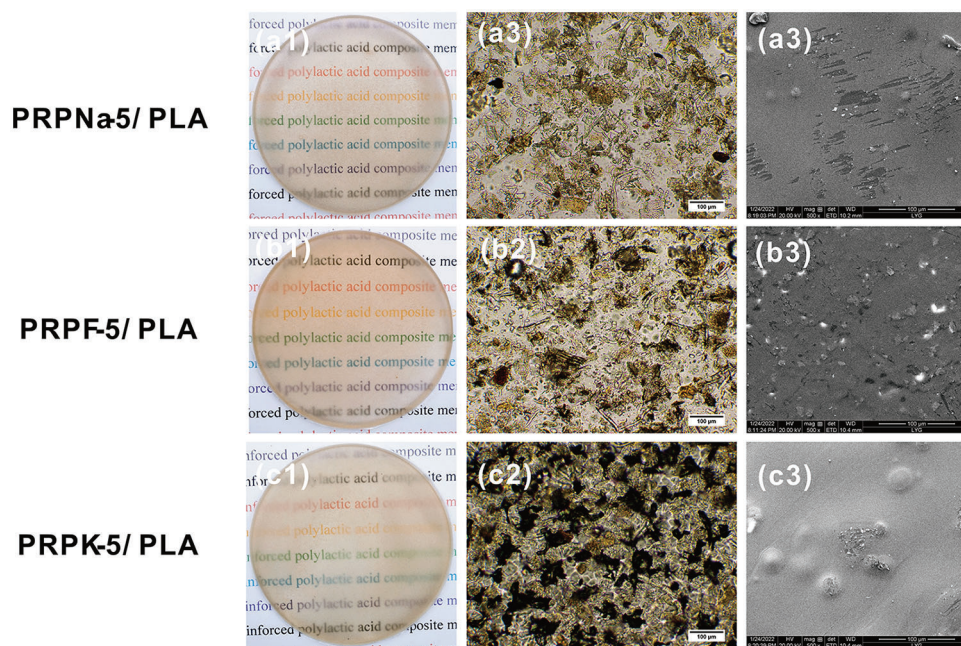
Figure 7: Photographs (left), optical microscope (center), and SEM image (right) of PLA composite films with treated PRP
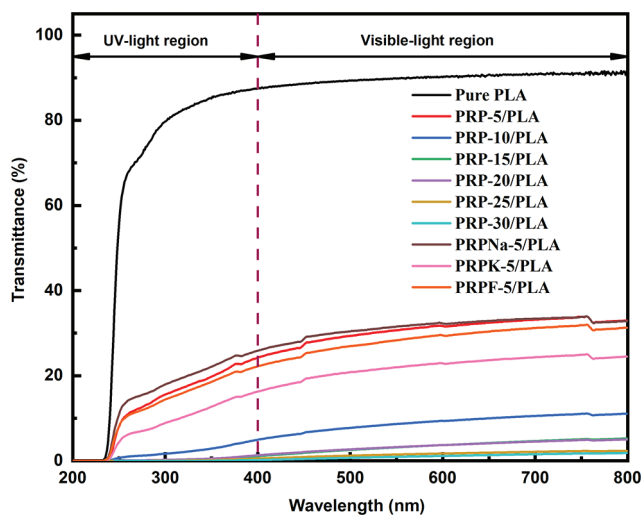

Figure 8: Light transmittance spectra of PRP/PLA

Table 5: UV transmittance of PRP/PLA biocomposite films

Sample	UVA 315–400 nm	UVB 280–315 nm	Transparency at λ_{800}(%) 800 nm
Pure PLA	93.1423	83.6851	89.3305
PRP-5/PLA	20.58569	15.14594	32.96097
PRP-10/PLA	3.281057	1.616704	11.09175

(Continued)

Table 5 (continued)

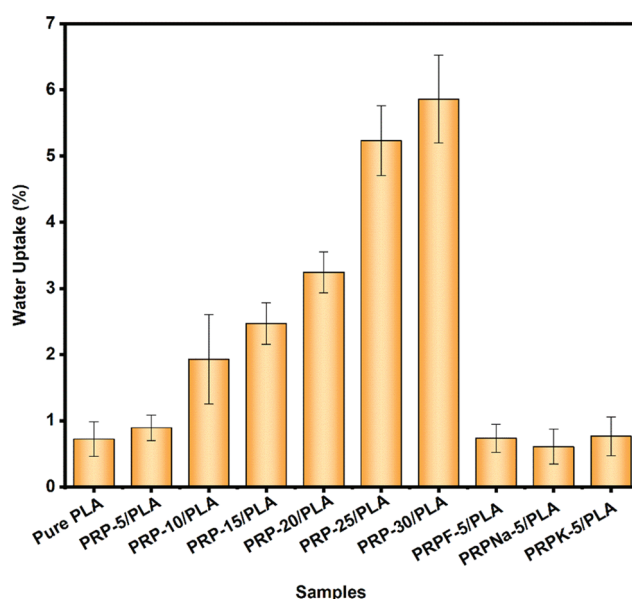| Sample	*UVA* 315–400 nm	*UVB* 280–315 nm	Transparency at λ_{800}(%) 800 nm
PRP-15/PLA	0.498361	0.111598	5.272299
PRP-20/PLA	0.688728	0.225235	5.023426
PRP-25/PLA	0.252092	0.062187	2.36592
PRP-30/PLA	0.073373	0.007828	1.845015
PRPNa-5/PLA	22.71996	17.58035	32.80953
PRPK-5/PLA	13.24895	8.606252	24.49063
PRPF-5/PLA	19.09673	14.03923	31.26079

Figure 9: Water absorption of pure PLA and PRP/PLA films

Compared with the PRP-5/PLA film, the W_a of the RPRK-5/PLA, PRPNa-5/PLA, and PRPF-5/PLA films reduced by 14%, 31.6%, and 17.4%, respectively. These results showed that formic acid, KH-550, and NaOH treatment reduced the number of hydroxyl groups on the surface of PRP. The reduced hydroxyl groups on the surface of PRP made PRP uniformly dispersed in the PLA matrix and made the surface of the composite films flatter and smoother, thus preventing water molecules from entering the composite films [49]. However, the surface treatment made the PRP surface rougher. The treatment promoted a stronger bond between PRP and PLA matrix, thereby preventing water molecules from diffusing through the gap between the fiber and the matrix [50]. The composite films had a low water absorption rate after surface treatment, close to that of pure PLA films. Thus the low absorption rate makes the composite films a great potential application for food packaging.

Although PRP/PLA film exhibits a low water absorption rate and is degradable, it can still be used as a packaging material for garment shopping, bread tote, and cookie overwrapping bags where water absorption

is insignificant. Paper bags have been widely used in the above areas, but they are brittle compared with PLA [51]. Moreover, Moy et al. also reported that PLA plastic is more environmentally friendly than paper [52].

3.7 Contact Angle of the Biocomposite Films

Fig. 10 shows the contact angle values of the untreated PLA and PRP/PLA composite films. The surficial characterization (hydrophobic and hydrophilic) of the films is essential in predicting the potential applications of these materials [18]. Hydrophobic or hydrophilic properties are often determined using surface energy and surface roughness. When the PRP content was low in PRP/PLA, the contact angle was mainly determined by the surface energy of the composite films. The pure PLA shows a contact angle value of 81.3°, whereas the contact angle value of PRP-5/PLA was close to 75.4°. This result was because the addition of PRP increased the polarity of PRP/PLA films, thus, enhancing the surface energy of the films and decreasing the contact angle [53]. In contrast, when the PRP content exceeded 5 wt%, the agglomeration of RPR increased, and the contact angle of the composite film was determined using surface energy and roughness. Thus, the contact angle of the composite film did not significantly correlate with PRP content [54].
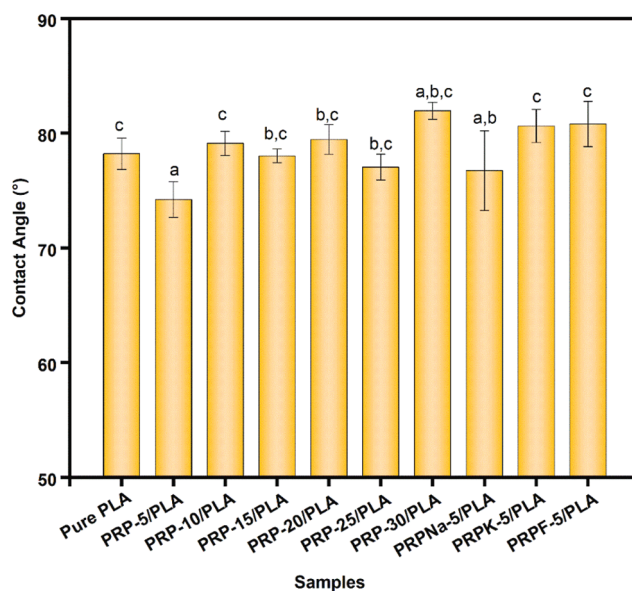

Figure 10: Contact angle of PRP/PLA films. Different characters above the columns indicate that there is a significant difference between samples at $p < 0.05$ (Student Newman Keuls test), same in the following figures

The results showed that the effect of NaOH treatment on the contact angle of PRP-5/PLA films was insignificant. The contact angle between PRPK-5/PLA and PRPF-5/PLA composite films was larger than that of PRP-5/PLA composite films. Because PRPK and PRPF were dispersed more uniformly in the PLA matrix, the number of hydroxyl groups exposed on the surface of the film was less. In addition, the modifier replaced the hydroxyl group in PRP, which reduced the hydrophilic of PRP, thus reducing the surface energy of the composite films.

3.8 Mechanical Properties of the Biocomposite Films

Young's modulus, elongation at break, and tensile strength of biocomposite films were measured, and the corresponding results are presented in Table 6 and Fig. 11. As the concentration of PRP increased, the

brittleness, tensile strain, and Young's modulus increased, decreased, and increased, respectively, consistent with the previous reports [18,27,55].
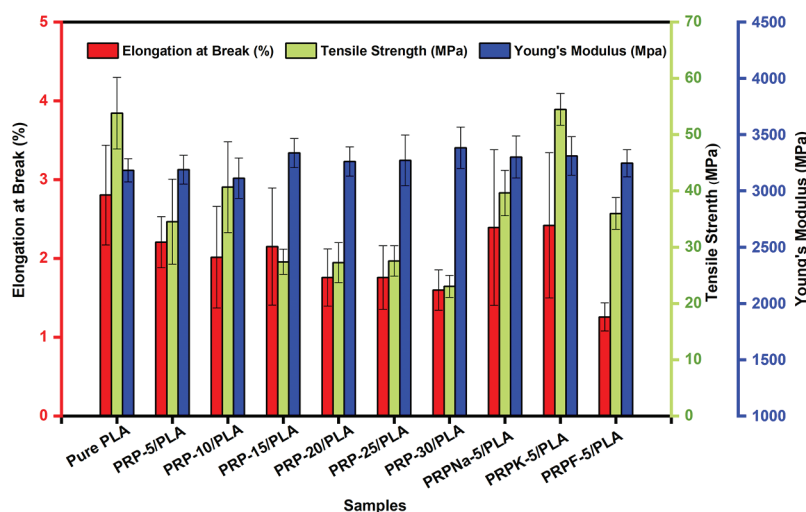

Figure 11: Tensile Strength, elongation at break, and Yong's modulus of PLA and PRP/PLA composite films

The addition of a specific amount of fiber increased the mechanical properties of PLA. When the fiber content exceeded this limit, the mechanical properties of the composite film deteriorated [56]. As shown in Fig. 11, PRP-10/PLA composite films showed a higher tensile strength (40.7 MP) than other biological composite films. When the content of PRP was less than 10 wt% (despite its good dispersibility), its crystallinity was significantly lower than that of the PRP-10/PLA film, thus reducing the tensile strength of the film. However, when the PRP content was more than 10 wt%, the tensile strength of the film decreased. As shown in Table 6, the tensile strengths of PRPNa-5/PLA, PRPF-5/PLA, and PRPK-5/PLA were significantly higher than the tensile strength of PRP-5/PLA. This phenomenon was attributed to the removal of moisture, wax, oil, lignin, and hemicellulose from the surface of PRP using formic acid and NaOH treatment, which made the surface of PRP rougher [20,30]. The interaction between PRP and PLA improved in proportion to the surface roughness, thus improving the tensile strength of PRP/PLA films. The chemical modification of natural fiber can improve the surface roughness of fiber and enhance the mechanical interaction between fiber and matrix [50].

Table 6: Mechanical properties of pure PLA and its composite films

Samples	Tensile strength/MPa	Elongation at break/%	Young's modulus/MPa
Pure PLA	53.4 ± 6.4^e	2.5 ± 0.8^{ab}	3184 ± 103^a
PRP-5/PLA	34.5 ± 7.6^d	2.2 ± 0.3^{ab}	3188 ± 128^a
PRP-10/PLA	40.7 ± 8.1^d	2.0 ± 0.6^{ab}	3112 ± 180^a
PRP-15/PLA	27.4 ± 2.2^{ab}	2.2 ± 0.7^{ab}	3337 ± 129^a
PRP-20/PLA	27.3 ± 3.5^{abc}	1.8 ± 0.4^{ab}	3261 ± 130^a
PRP-25/PLA	27.6 ± 2.7^{ab}	1.8 ± 0.4^{ab}	3271 ± 225^a
PRP-30/PLA	23.0 ± 1.9^a	1.6 ± 0.2^a	3383 ± 184^a
PRPNa-5/PLA	39.6 ± 4.0^d	2.8 ± 1.3^b	3301 ± 187^a
PRPK-5/PLA	54.5 ± 2.8^e	2.8 ± 1.2^b	3310 ± 171^a
PRPF-5/PLA	36.0 ± 2.8^{cd}	1.5 ± 0.5^a	3246 ± 120^a

However, no significant difference was observed in Young's modulus of the PRP/PLA films (Table 6). These results were consistent with that of Geng et al. that the incorporation of fiber and graft-modified fiber had little effect on Young's modulus of PLA [57], indicating that Young's Modulus of the PRP/PLA films was mainly controlled by the alignment of PLA chains [57].

The elongation at break of pure PLA composite films was higher than those of unmodified PRP/PLA composite films because the addition of PRP impeded the movement of PLA chains, thus enhancing the rigidity of PRP/PLA composite films [20].

Comparing all results in this study, the PRPK-5/PLA films exhibited superior mechanical properties: Young's modulus, elongation at break, and tensile strength. These superior results were attributed to the effective reaction of the KH-550 molecule with the hydroxyl group on the surface of PRP to form an ordered coupling agent monolayer. In addition, the hydrophobicity of PRP increased, thereby improving the compatibility of PRP and PLA [34]. Moreover, the results showed that the treatment of PRP with KH-550 modified PRP surface, thus improving the interaction in the interface region between the PLA matrix and fibers, indicating that the PRPK-5/PLA composite films are promising biodegradable alternative to common polymers for food packaging.

3.9 Soil Degradability of the Biocomposite Films

The changes in the prepared films were studied by measuring the weight loss and examining the morphological changes in the polymeric material as they degraded in soil for 40 days. As shown in Fig. 12, the transparency of the composite film decreased after it was buried in the soil, and the brittleness of the composite film increased with the increase in PRP content. A similar phenomenon was observed by Bayerl et al. [58].
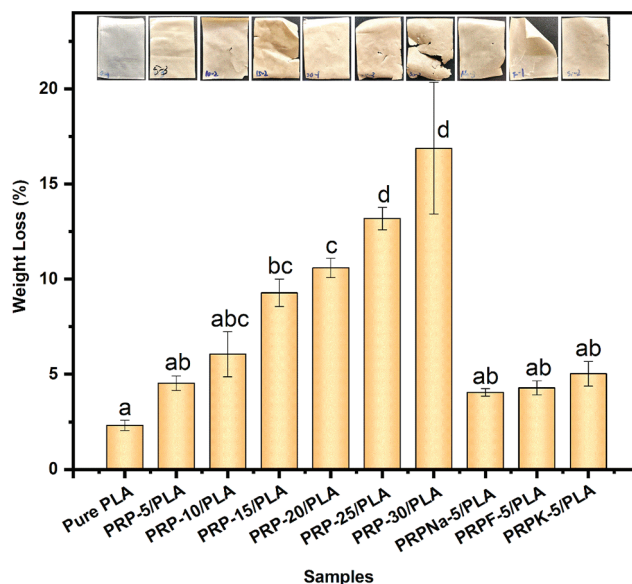

Figure 12: The mass loss histogram of pure PLA and its composite films degraded in the soil after 40 days

The weight loss of all composite films was higher than that of pure PLA films, and pure PLA composite films lost 2.31% of their weight within 40 days of degradation. The degradation of pure PLA composite films was divided into two steps. First, the ester groups were hydrolyzed to form a low molecular weight substance.

Second, when the hydrolysis reached a certain level, enzyme degradation occurred and degraded small molecules to carbon dioxide and water [59].

The degradation rate of the composite film increased in proportion to the PRP content. A weight loss of 16.88% was observed when the PRP content was 30 wt%. Cracks were also observed on the surface of composite film containing high PRP content because the PRP acted as a conduit for transporting water and microorganisms from the exterior to the interior of the composite film. The water molecules and microorganisms accelerated the degradation of PLA composite films, with only marginal degradation occurring on the exterior surface of pure PLA composite films [59]. The hydroxyl group in cellulose catalyzed the hydrolysis of PLA ester groups, thereby accelerating the decomposition of PLA [60]. The presence of fibers caused the swelling of the composite film, with 30 wt% having the highest water uptake and the greatest weight loss at 24 h [17]. Thus, the presence of fibers also promotes the degradation of PLA.

As shown in Fig. 12, chemical modifications on RPR had little effect on the composite film degradability. Compared with the unmodified PRP/PLA film, the addition of PRPNa and PRPF slowed down the degradation rate of the composite film buried in the soil. As previously noted, the hydroxyl groups on the surface of modified PRP were reduced, thus reducing the water absorption and degradation of PLA. Moreover, the compatibility between the modified PRP and the PLA matrix was good, and fewer cavities and voids at the interface were observed, which was consistent with the observation of Gisan et al. [20].

4 Conclusions

In this study, PRP/PLA composite films were prepared via a solution casting method, and the main results and conclusions were summarized as follows:

1. The addition of surface-treated PRP to PLA increased the toughness of PLA. When the addition of PRPK was 5 wt%, the tensile strength, elongation at break, and Young's modulus of the composite film increased to 54.5 MPa, 2.8%, and 3310 MPa, respectively.

2. The PRP had a significant positive effect on the thermal stability, UV resistance, and biodegradability of the PLA composite films. Compared to pure PLA film, the T_{onset} of the film with 5 wt% PRP increased from 339°C to 341°C. With the increasing PRP content in the composite films, the UV resistance of the composite films became stronger, and the UVA and UVB values of the composite film were almost 0 when the PRP content was 15 wt%. The PRP improved the swelling performance of the composite film and increased the access of PLA to water and bacteria, thereby increasing the degradability of the composite film in soil. The composite film lost weight when the PRP content was 30 wt%, which was 7.3 times that of pure PLA composite film.

3. PRP (5 wt%) exhibited the best enhancement effect on the composite film. PRP-5 improved the thermal stability, UV resistance, and biodegradability of the composite film. Compared with NaOH and formic acid treatments, the KH-550 treatment exhibited a better modification effect on PRP.

4. This study only explored the effects of modified PRP (5 wt%) on the composite film performance. The effects of modified PRP of other contents on composite film performance needs further research.

Conflicts of Interest: The authors declare that they have no conflicts of interest to report regarding the present study.

References

1. Acquavia, M. A., Pascale, R., Martelli, G., Bondoni, M., Bianco, G. (2021). Natural polymeric materials: A solution to plastic pollution from the agro-food sector. *Polymers, 13(1),* 158. https://doi.org/10.3390/polym13010158

2. Li, K. Q., Chen, Y., Liu, J. C., Zhang, L., Mu, X. W. (2021). Online food delivery platforms and restaurants' interactions in the context of the ban on using single-use plastics. *IEEE Access, 9,* 96210–96220. https://doi.org/10.1109/ACCESS.2021.3095296

3. Mendes, A. C., Pedersen, G. A. (2021). Perspectives on sustainable food packaging:- is bio-based plastics a solution? *Trends in Food Science & Technology, 112(1),* 839–846. https://doi.org/10.1016/j.tifs.2021.03.049

4. Niu, X., Liu, Y. T., Song, Y., Han, J. Q., Pan, H. (2018). Rosin modified cellulose nanofiber as a reinforcing and co-antimicrobial agents in polylactic acid/chitosan composite film for food packaging. *Carbohydrate Polymers, 183(5),* 102–109. https://doi.org/10.1016/j.carbpol.2017.11.079

5. Murariu, M., Dubois, P. (2016). PLA composites: From production to properties. *Advanced Drug Delivery Reviews, 107,* 17–46. https://doi.org/10.1016/j.addr.2016.04.003

6. Brounstein, Z., Yeager, C. M., Labouriau, A. (2021). Development of antimicrobial PLA composites for fused filament fabrication. *Polymers, 13(4),* 580. https://doi.org/10.3390/polym13040580

7. Mangaraj, S., Yadav, A., Bal, L. M., Dash, S. K., Mahanti, N. K. (2018). Application of biodegradable polymers in food packaging industry: A comprehensive review. *Journal of Packaging Technology and Research, 3(1),* 77–96. https://doi.org/10.1007/s41783-018-0049-y

8. Naser, A. Z., Deiab, I., Defersha, F., Yang, S. (2021). Expanding poly(lactic acid) (PLA) and polyhydroxyalkanoates (PHAs) applications: A review on modifications and effects. *Polymers, 13(23),* 4271. https://doi.org/10.3390/polym13234271

9. Rajeshkumar, G., Seshadri, S. A., Devnani, G. L., Sanjay, M. R., Siengchin, S. et al. (2021). Environment friendly, renewable and sustainable poly lactic acid (PLA) based natural fiber reinforced composites-a comprehensive review. *Journal of Cleaner Production, 310(1),* 127483. https://doi.org/10.1016/j.jclepro.2021.127483

10. Singha, S., Hedenqvist, M. S. (2020). A review on barrier properties of poly(lactic acid)/clay nanocomposites. *Polymers, 12(5),* 1095. https://doi.org/10.3390/polym12051095

11. Zamir, S. S., Fathi, B., Ajji, A., Robert, M., Elkoun, S. (2022). Biodegradation of modified starch/poly lactic acid nanocomposite in soil. *Polymer Degradation and Stability, 199,* 109902. https://doi.org/10.1016/j.polymdegradstab.2022.109902

12. Zhou, L., Ke, K., Yang, M. B., Yang, W. (2021). Recent progress on chemical modification of cellulose for high mechanical-performance poly(lactic acid)/cellulose composite: A short review. *Composites Communications, 23,* 100548. https://doi.org/10.1016/j.coco.2020.100548

13. Cui, X. N., Ozaki, A., Asoh, T. A., Uyama, H. (2020). Cellulose modified by citric acid reinforced poly(lactic acid) resin as fillers. *Polymer Degradation and Stability, 175,* 109118. https://doi.org/10.1016/j.polymdegradstab.2020.109118

14. Yang, R. Y., Wang, D. Y., Li, H. L., He, Y., Zheng, X. Y. et al. (2019). Preparation and characterization of *Bletilla striata* polysaccharide/polylactic acid composite. *Molecules, 24(11),* 2104. https://doi.org/10.3390/molecules24112104

15. Yang, Y., Zhang, L. S., Xiong, Z., Tang, Z. B., Zhang, R. Y. et al. (2016). Research progress in the heat resistance, toughening and filling modification of PLA. *Science China Chemistry, 59(11),* 1355–1368. https://doi.org/10.1007/s11426-016-0222-7

16. Soleimanian, Y., Sanou, I., Turgeon, S. L., Canizares, D., Khalloufi, S. (2022). Natural plant fibers obtained from agricultural residue used as an ingredient in food matrixes or packaging materials: A review. *Comprehensive Reviews in Food Science and Food Safety, 21(1),* 371–415. https://doi.org/10.1111/1541-4337.12875

17. Papadopoulou, E. L., Paul, U. C., Tran, T. N., Suarato, G., Ceseracciu, L. et al. (2019). Sustainable active food packaging from poly(lactic acid) and cocoa bean shells. *ACS Applied Materials & Interfaces, 11(34),* 31317–31327. https://doi.org/10.1021/acsami.9b09755

18. Silva, C. G., Campini, P. A. L., Rocha, D. B., Rosa, D. S. (2019). The influence of treated *Eucalyptus* microfibers on the properties of PLA biocomposites. *Composites Science and Technology, 179,* 54–62. https://doi.org/10.1016/j.compscitech.2019.04.010

19. Getmea, A. S., Patelb, B. (2020). A review: Bio-fiber's as reinforcement in composites of polylactic acid (PLA). *Materials Today: Proceedings, 26,* 2116–2122. https://doi.org/10.1016/j.matpr.2020.02.457

20. Gisan, K. A., Chan, M. Y., Koay, S. C. (2022). Solvent-cast biofilm from poly(lactic) acid and durian husk fiber: Tensile, water absorption, and biodegradation behaviors. *Journal of Natural Fibers, 19(11)*, 4338–4349. https://doi.org/10.1080/15440478.2020.1857894

21. Yin, L., Chen, X., Li, N., Jia, W. H., Wang, N. Q. et al. (2021). *Puerarin* ameliorates skeletal muscle wasting and fiber type transformation in STZ-induced type 1 diabetic rats. *Biomedicine & Pharmacotherapy, 133,* 110977. https://doi.org/10.1016/j.biopha.2020.110977

22. Zhang, Q. R., Wang, C. G., Ji, D. Y., Liu, Y. Y. (2011). Research on preparing natural puerariae fiber from puerariae residues. *Shanghai Textile Science & Technology, 39(2),* 26–28. https://doi.org/10.16549/j.cnki.issn.1001-2044.2011.02.011

23. Li, M. H., Han, G. T., Song, Y., Jiang, W., Zhang, Y. M. (2016). Structure, composition, and thermal properties of cellulose fibers from *Pueraria lobata* treated with a combination of steam explosion and laccase mediator system. *Bioresources, 11(3),* 6854–6866. https://doi.org/10.15376/biores.11.3.6854-6866

24. Adel, A. M., El-Wahab, Z. H. A., Ibrahim, A. A., Al-Shemy, M. T. (2011). Characterization of microcrystalline cellulose prepared from lignocellulosic materials. Part II: Physicochemical properties. *Carbohydrate Polymers, 83(2),* 676–687. https://doi.org/10.1016/j.carbpol.2010.08.039

25. Ibrahim, M. M., El-Zawawy, W. K., Juttke, Y., Koschella, A., Heinze, T. (2013). Cellulose and microcrystalline cellulose from rice straw and banana plant waste: Preparation and characterization. *Cellulose, 20(5),* 2403–2416. https://doi.org/10.1007/s10570-013-9992-5

26. Wang, Y. C., Liu, S. S., Wang, Q., Ji, X. X., Yang, G. H. et al. (2021). Strong, ductile and biodegradable polylactic acid/lignin-containing cellulose nanofibril composites with improved thermal and barrier properties. *Industrial Crops and Products, 171,* 113898. https://doi.org/10.1016/j.indcrop.2021.113898

27. Sucinda, E. F., Majid, M. S. A., Ridzuan, M. J. M., Cheng, E. M., Alshahrani, H. A. et al. (2021). Development and characterisation of packaging film from napier cellulose nanowhisker reinforced polylactic acid (PLA) bionanocomposites. *International Journal of Biological Macromolecules, 187,* 43–53. https://doi.org/10.1016/j.ijbiomac.2021.07.069

28. Wang, D., Bai, T., Cheng, W. L., Xu, C., Wang, G. et al. (2019). Surface modification of bamboo fibers to enhance the interfacial adhesion of epoxy resin-based composites prepared by resin transfer molding. *Polymers, 11(12),* 2107. https://doi.org/10.3390/polym11122107

29. Turco, R., Zannini, D., Mallardo, S., Dal Poggetto, G., Tesser, R. et al. (2021). Biocomposites based on poly(lactic acid), cynara cardunculus seed oil and fibrous presscake: A novel eco-friendly approach to hasten PLA biodegradation in common soil. *Polymer Degradation and Stability, 188(1),* 109576. https://doi.org/10.1016/j.polymdegradstab.2021.109576

30. Wu, R. C., Zhao, X. B., Liu, D. H. (2016). Structural features of formiline pretreated sugar cane bagasse and their impact on the enzymatic hydrolysis of cellulose. *ACS Sustainable Chemistry & Engineering, 4(3),* 1255–1261. https://doi.org/10.1021/acssuschemeng.5b01298

31. Long, S. Y., Zhong, L., Lin, X. L., Chang, X. G., Wu, F. Q. et al. (2021). Preparation of formyl cellulose and its enhancement effect on the mechanical and barrier properties of polylactic acid films. *International Journal of Biological Macromolecules, 172,* 82–92. https://doi.org/10.1016/j.ijbiomac.2021.01.029

32. Jin, K. Y., Tang, Y. J., Zhu, X. M., Zhou, Y. M. (2020). Polylactic acid based biocomposite films reinforced with silanized nanocrystalline cellulose. *International Journal of Biological Macromolecules, 162,* 1109–1117. https://doi.org/10.1016/j.ijbiomac.2020.06.201

33. Wang, Q. T., Zhang, Y., Liang, W. K., Wang, J. J., Chen, Y. X. (2020). Effect of silane treatment on mechanical properties and thermal behavior of bamboo fibers reinforced polypropylene composites. *Journal of Engineered Fibers and Fabrics, 15,* 1–10. https://doi.org/10.1177/1558925020958195

34. Li, X., Deng, L. G., Li, Y., Li, K. (2020). Preparation of microcrystalline cellulose from bagasse bleached pulp reinforced polylactic acid composite films. *Sugar Tech, 22(6),* 1138–1147. https://doi.org/10.1007/s12355-020-00827-w

35. Xiao, W. L., Niu, B. H., Yu, M., Sun, C. D., Wang, L. H. et al. (2021). Fabrication of foam-like oil sorbent from polylactic acid and *Calotropis gigantea* fiber for effective oil absorption. *Journal of Cleaner Production, 278,* 123507. https://doi.org/10.1016/j.jclepro.2020.123507

36. Sneha, K. R., Steny, P. S., Sailaja, G. S. (2021). Intrinsically radiopaque and antimicrobial cellulose based surgical sutures from mechanically powerful *Agave sisalana* plant leaf fibers. *Biomaterials Science, 9(23),* 7944–7961. https://doi.org/10.1039/D1BM01316E

37. Ozyhar, T., Baradel, F., Zoppe, J. (2020). Effect of functional mineral additive on processability and material properties of wood-fiber reinforced poly(lactic acid) (PLA) composites. *Composites Part A–Applied Science and Manufacturing, 132,* 105827. https://doi.org/10.1016/j.compositesa.2020.105827

38. Li, X., Tabil, L. G., Panigrahi, S. (2007). Chemical treatments of natural fiber for use in naturalfiber-reinforced composites: A review. *Journal of Polymers and the Environment, 15(1),* 25–33. https://doi.org/10.1007/s10924-006-0042-3

39. Yang, Z. Z., Feng, X. H., Xu, M., Rodrigue, D. (2020). Properties of poplar fiber/PLA composites: Comparison on the effect of maleic anhydride and kh550 modification of poplar fiber. *Polymers, 12(3),* 729. https://doi.org/10.3390/polym12030729

40. Momeni, S., Safder, M., Khondoker, M. A., Elias, A. L. (2021). Valorization of hemp hurds as bio-sourced additives in PLA-based biocomposites. *Polymers, 13(21),* 3786. https://doi.org/10.3390/polym13213786

41. Suryanegara, L., Nakagaito, A. N., Yano, H. (2009). The effect of crystallization of PLA on the thermal and mechanical properties of microfibrillated cellulose-reinforced PLA composites. *Composites Science and Technology, 69(7–8),* 1187–1192. https://doi.org/10.1016/j.compscitech.2009.02.022

42. Woo, E. M., Lugito, G. (2016). Cracks in polymer spherulites: Phenomenological mechanisms in correlation with ring bands. *Polymers, 8(9),* 329. https://doi.org/10.3390/polym8090329

43. Pan, F. Y., Chen, L., Jiang, Y. Z., Xiong, L., Min, L. et al. (2018). Bio-based UV protective films prepared with polylactic acid (PLA) and *Phoebe zhennan* extractives. *International Journal of Biological Macromolecules, 119,* 582–587. https://doi.org/10.1016/j.ijbiomac.2018.07.189

44. Kale, R. D., Gorade, V. G., Madye, N., Chaudhary, B., Bangde, P. S. et al. (2018). Preparation and characterization of biocomposite packaging film from poly(lactic acid) and acylated microcrystalline cellulose using rice bran oil. *International Journal of Biological Macromolecules, 118,* 1090–1102. https://doi.org/10.1016/j.ijbiomac.2018.06.076

45. Wang, Z. H., Yao, Z. J., Zhou, J. T., He, M., Jiang, Q. et al. (2019). Improvement of polylactic acid film properties through the addition of cellulose nanocrystals isolated from waste cotton cloth. *International Journal of Biological Macromolecules, 129,* 878–886. https://doi.org/10.1016/j.ijbiomac.2019.02.021

46. Oliver-Ortega, H., Tarres, Q., Mutje, P., Delgado-Aguilar, M., Mendez, J. A. et al. (2020). Impact strength and water uptake behavior of bleached kraft softwood-reinforced PLA composites as alternative to PP-based materials. *Polymers, 12(9),* 2144. https://doi.org/10.3390/polym12092144

47. Jiang, N., Li, Y. M., Li, Y. K., Yu, T., Li, Y. et al. (2020). Effect of short jute fibers on the hydrolytic degradation behavior of poly(lactic acid). *Polymer Degradation and Stability, 178,* 109214. https://doi.org/10.1016/j.polymdegradstab.2020.109214

48. Yew, G. H., Mohd Yusof, A. M., Mohd Ishak, Z. A., Ishiaku, U. S. (2005). Water absorption and enzymatic degradation of poly(lactic acid)/rice starch composites. *Polymer Degradation and Stability, 90(3),* 488–500. https://doi.org/10.1016/j.polymdegradstab.2005.04.006

49. Hussain, A., Blanchet, P. (2021). Preparation of breathable cellulose based polymeric membranes with enhanced water resistance for the building industry. *Materials, 14(15),* 4310. https://doi.org/10.3390/ma14154310

50. Nanthakumar, K., Yeng, C. M., Chun, K. S. (2020). Tensile and water absorption properties of solvent cast biofilms of sugarcane leaves fibre-filled poly(lactic) acid. *Journal of Thermoplastic Composite Materials, 33(3),* 289–304. https://doi.org/10.1177/0892705718805526

51. Niu, X., Huan, S., Li, H., Pan, H., Rojas, O. J. (2021). Transparent films by ionic liquid welding of cellulose nanofibers and polylactide: Enhanced biodegradability in marine environments. *Journal of Hazardous Materials, 402(9),* 124073. https://doi.org/10.1016/j.jhazmat.2020.124073

52. Moy, C. H., Tan, L. S., Shoparwe, N. F., Shariff, A. M., Tan, J. (2021). Comparative study of a life cycle assessment for bio-plastic straws and paper straws: Malaysia's perspective. *Processes, 9(6),* 9061007. https://doi.org/10.3390/pr9061007

53. El Assimi, T., Blazic, R., Vidovic, E., Raihane, M., El Meziane, A. et al. (2021). Polylactide/cellulose acetate biocomposites as potential coating membranes for controlled and slow nutrients release from water-soluble fertilizers. *Progress in Organic Coatings, 156,* 106255. https://doi.org/10.1016/j.porgcoat.2021.106255

54. Jamaluddin, N., Kanno, T., Asoh, T. A., Uyama, H. (2019). Surface modification of cellulose nanofiber using acid anhydride for poly(lactic acid) reinforcement. *Materials Today Communications, 21,* 100587. https://doi.org/10.1016/j.mtcomm.2019.100587

55. Gazzotti, S., Rampazzo, R., Hakkarainen, M., Bussini, D., Ortenzi, M. A. et al. (2019). Cellulose nanofibrils as reinforcing agents for PLA-based nanocomposites: An *in situ* approach. *Composites Science and Technology, 171,* 94–102. https://doi.org/10.1016/j.compscitech.2018.12.015

56. Ma, Y. R., Qian, S. P., Hu, L., Qian, J., Lopez, C. A. F. et al. (2018). Mechanical, thermal, and morphological properties of PLA biocomposites toughened with silylated bamboo cellulose nanowhiskers. *Polymer Composites, 40(8),* 3012–3019. https://doi.org/10.1002/pc.25144

57. Geng, S. Y., Yao, K., Zhou, Q., Oksman, K. (2018). High-strength, high-toughness aligned polymer-based nanocomposite reinforced with ultralow weight fraction of functionalized nanocellulose. *Biomacromolecules, 19(10),* 4075–4083. https://doi.org/10.1021/acs.biomac.8b01086

58. Bayerl, T., Geith, M., Somashekar, A. A., Bhattacharyya, D. (2014). Influence of fibre architecture on the biodegradability of FLAX/PLA composites. *International Biodeterioration & Biodegradation, 96,* 18–25. https://doi.org/10.1016/j.ibiod.2014.08.005

59. Hakkarainen, M., Albertsson, A., Karlsson, S. (1996). Weight losses and molecular weight changes correlated with the evolution of hydroxyacids in simulated *in vivo* degradation of homo and copolymers of PLA and PG. *Polymer Degradation and Stability, 52(3),* 283–291. https://doi.org/10.1016/0141-3910(96)00009-2

60. Fortunati, E., Puglia, D., Monti, M., Santulli, C., Maniruzzaman, M. et al. (2013). Okra (*Abelmoschus esculentus*) fibre based PLA composites: Mechanical behaviour and biodegradation. *Journal of Polymers and the Environment, 21(3),* 726–737. https://doi.org/10.1007/s10924-013-0571-5